QUADRUPOLAR EFFECTS IN THE NMR SPECTRUM OF ^{51}V IN $DyVO_4$

ELECTRIC QUADRUPOLE EFFECTS ON THE ANGULAR DEPENDENCE OF THE NMR SPECTRUM OF ^{51}V IN $DyVO_4$ AT T=292°K AND T=77°K

By

WILLIAM PATRICK JEEVES, B.Sc.

A Thesis

Submitted to the School of Graduate Studies

in Partial Fulfilment of the Requirements

for the Degree

Master of Science

McMaster University

September, 1975

© WILLIAM PATRICK JEEVES 1977

MASTER OF SCIENCE (1975) McMaster University
(Physics) Hamilton, Ontario

TITLE: The Investigation of the Temperature Dependence of the NMR Spectrum of ^{51}V in $DyVO_4$ by Study of its Electric Quadrupole Interaction Induced Angular Variation at T=77°K and T=292°K

AUTHOR: William Patrick Jeeves, B.Sc. (McMaster University)

SUPERVISOR: Professor C. V. Stager

NUMBER OF PAGES:

ABSTRACT

The nuclear magnetic resonance spectrum of the ^{51}V nucleus in $DyVO_4$ has been investigated in order to determine if the crystal undergoes any crystallographic distortion or symmetry reduction down to liquid nitrogen temperature, T=77°K. It has been found, using the effects of the electric quadrupole interaction at the vanadium nucleus, that no such distortion or symmetry alteration could be detected down to T=77°K. Although it is known that the crystal undergoes a spontaneous second-order crystallographic phase transition, via the cooperative Jahn-Teller effect , to a state of lower symmetry at a temperature T_D=14°K , and that it undergoes a second transition to an antiferromagnetic state at T_N=3.04°K , these phenomena were unfortunately unable to be observed due to technical difficulties. However, the existence and effects of the electric quadrupole interaction in $DyVO_4$ at T=77°K and T=292°K have been established, and speculation has been made as to the possible findings in the very low temperature range between 2°K and 15°K.

ACKNOWLEDGEMENTS

I would first and foremost like to express my sincere gratitude to my supervisor, Dr. Carl Stager, not only for his expert assistance in the performing of the NMR experiments, but also in the correct and careful analysis of the data. I thank him for his willingness to help at all times, as well as for his enduring patience. I have also learned from him that elaborate literary prose, written in the first person plural, is not the most suitable mode of expression of scientific communication, nor of the elucidation of numerical physical quantities.

My special thanks go to John Neimanis for his technical assistance during some of the experiments. My thanks are also due to him, as well as to Judy Hall, for the acquisition and analysis of the magnetization data necessary for the analysis of the NMR results, and I thank David Montgomery for his work on the non-linear least squares program used in this work.

I very much want to thank all the good friends I have made during my stay in the East basement wing of Senior Sciences, Fred Long, Brian Farnworth, Dave Sanders, Ed Kwasniewski, Bob Lendrum, again John Neimanis as well as both Bill and Judy Hall, without whom this work would more

than likely have been possible, but who made it both enjoyable and worthwhile. Some of them more than others I should thank for not only a better understanding of the classical mechanics of the game of billiards, as well as the fundamental underlying principles of softball, but also for a hastening of the onset of cirrhosis of the liver. The latter phenomenon seems to display quite definite cooperative humanoid characteristics, and is still under intensive study (private communication).

Needless to say, I owe my wife, Dorisanne, a word of appreciation for her extreme patience, especially during the latter stages of the preparation of the thesis, as well as for the typing of the good rough copy, my handwriting being totally illegible. I would like to thank her for marrying me in the first place, for the last few months would have been far less easy to bear without her.

Lastly, I would very much like to thank not only Mr. David Hodgson for the diagrams that are in this work, but also Mrs. Murlis Pope for having typed this thesis with as much patience and perseverence as I am sure it must have taken.

TABLE OF CONTENTS

LIST OF FIGURES

LIST OF TABLES

CHAPTER I

INTRODUCTION

The rare-earth vanadates, phosphates, and arsenates, which crystallize in the tetragonal zircon structure [1], have very interesting properties at low temperatures. Dysprosium vanadate, $DyVO_4$, in particular, at very low temperatures, i.e. below 3.04°K [2], orders antiferromagnetically[3] with the direction of the magnetic moments perpendicular to the optical or c-axis. It is of interest to note that $DyVO_4$ undergoes a second-order crystallographic phase transition to a lower symmetry at a temperature T_D = 14° K[4], well above the Neel temperature T_N, induced by what is known as a cooperative Jahn-Teller effect. A result of this distortion is that the lowest crystal field components of the rare-earth ground level are split. That is, at temperatures well below T_D, the lowest lying crystal field components of $DyVO_4$ form a doublet or quasi-doublet, which has a very large magnetic moment (g factor) in a special direction in the basal plane perpendicular to the c-axis.

In this work, the nuclear magnetic resonance (NMR) spectrum of the vanadium nucleus in $DyVO_4$ is investigated with a view to determining the extent of the distortion or symmetry alteration down to T = 77°K (liquid nitrogen temperature).

This information is revealed by the electric quadrupole interaction at the vanadium nucleus. The latter effect occurs due to the fact that the vanadium nucleus has an electric quadrupole moment and is surrounded by an oxygen 'cage'. This oxygen 'cage', as will be seen, produces an electric field gradient at the vanadium nucleus. The NMR spectrum permits us to determine the magnitude of this quadrupole interaction, and the temperature dependence of the spectrum therefore gives us an indication of the temperature variation of the interaction.

Due to the second-order phase transition, mentioned above, it would be of obvious interest to investigate the vanadium NMR spectrum at temperatures close to T_N but below T_D, as well as just above T_D. This would provide a measure of the symmetry reduction and crystallographic distortion that occurs. Such a distortion, resulting in the splitting of an otherwise degenerate ground level of the crystal, would not only lead to an altered value of the electric field gradient at the vanadium site, but would also lead to substantial changes in the interaction between the paramagnetic dysprosium ions and the vanadium nuclei. In Chapter II the effect of this interaction on the NMR spectra will be presented.

Unfortunately, however, difficulties of a technical nature do not permit at this time a study of these effects at such low temperatures, but only down to T = 77°K.

A crystallographic description of the $DyVO_4$ crystal is at this point worth giving. $DyVO_4$ is one of the rare-earth vanadates, having the body-centred tetragonal structure, with four molecular units per conventional tetragonal unit cell above

the Jahn-Teller transition temperature T_D. At 77°K the lattice parameters are:

$$a = b = 7.1434 \text{ Å},$$
$$c = 6.3130 \text{ Å}. \quad (5)$$

The structure is a typical zircon structure with space group I_{41}/amd [6] above T_D.

The paramagnetic Dy^{3+} ions occupy the positions $(0,0,0)$; $(0,\frac{1}{2},\frac{1}{4})$; $(\frac{1}{2},\frac{1}{2},\frac{1}{2})$; $(\frac{1}{2},0,\frac{3}{4})$ in the unit cell, (see Fig. I). These ions have electronic structure $4s^2\ 4p^6\ 4d^{10}\ 4f^9$. The V^{5+} ions, on the other hand, occupy the positions $(0,0,\frac{1}{2})$; $(0,\frac{1}{2},\frac{3}{4})$; $(\frac{1}{2},\frac{1}{2},0)$; $(\frac{1}{2},0,\frac{1}{4})$. From symmetry, all vanadium ion sites are magnetically and structurally equivalent, and each V^{5+} ion is located at the centre of a slightly distorted tetrahedron of four oxygen ions, each of which lies at a distance of 1.72 Å from the V^{5+} ion.

Because of the presence of the Dy^{3+} ions, the sample acquires a paramagnetic magnetization when it is subjected to an external static magnetic field. The interaction between the paramagnetic moments and the vanadium nuclei is an important factor in determining the NMR spectrum. Vanadium has only one stable isotope, ^{51}V, with $I = \frac{7}{2}$. The magnitude of the electric quadrupole moment Q_V is equal to -0.05×10^{-24} cm^2. Since the oxygen tetrahedron is not a perfect one, we therefore expect a non-vanishing electric field gradient at the vanadium nucleus site. This will lead to an electric quadrupole interaction between Q_V and the environmental electric field gradient. The interaction energy depends, as will be seen in the next chapter, on the orientation of the nuclear spin.

Fig. 1

Perspective 3-D diagram of the $DyVO_4$ crystal. The large circles represent the Dy^{3+} ions, while the tetrahedra containing the smaller circles represent the VO_4^{3-} complexes. The oxygen atoms are to be thought of as being at the corners of the tetrahedra, while the vanadium atoms are shown by the small circles at the centres of the tetrahedra.

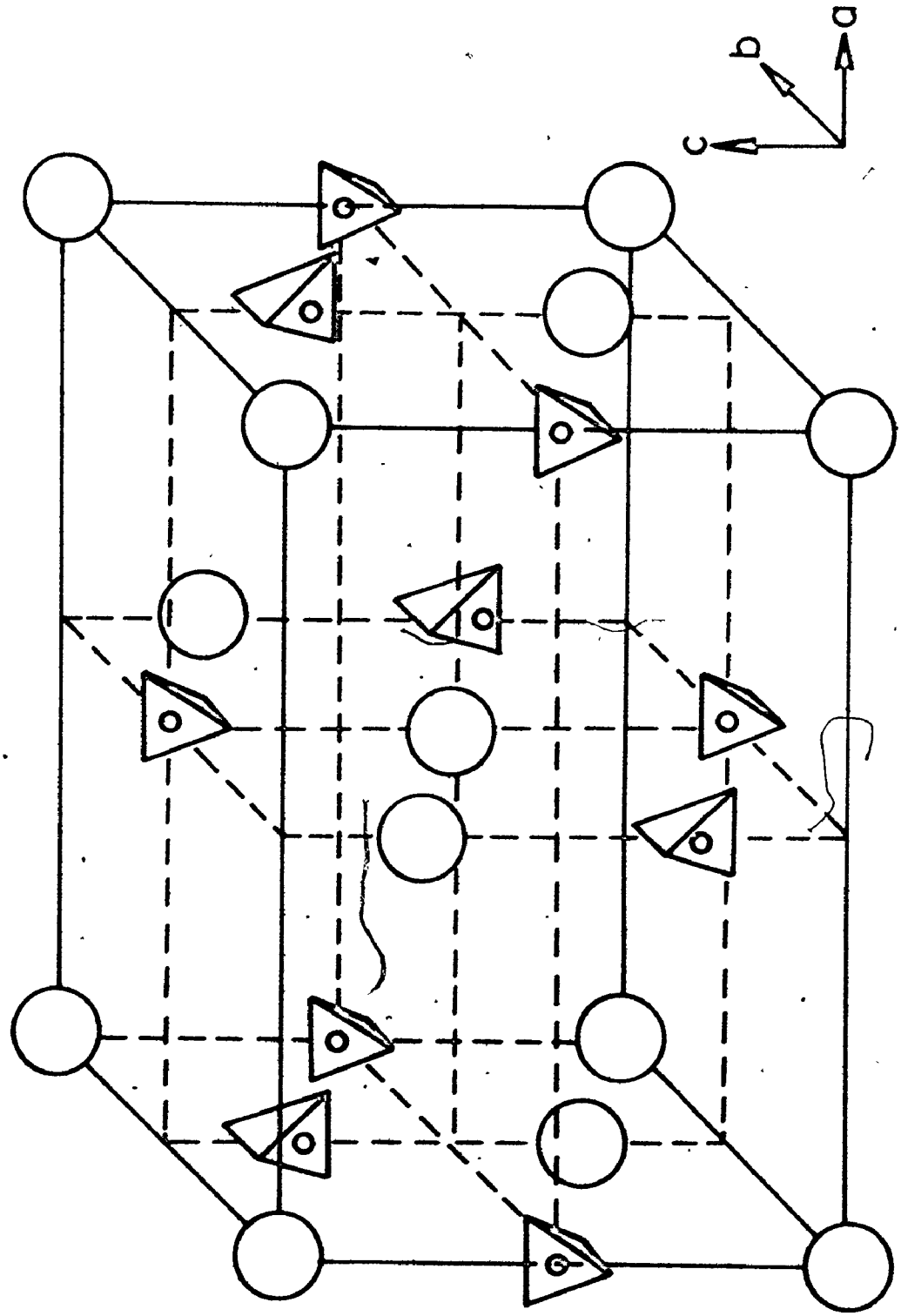
a
b
c

In Chapter II, the general Hamiltonian of the vanadium nucleus, embedded in a crystal of $DyVO_4$, is developed and various parameters of interest established. This chapter also contains a description of the angular dependence of the nuclear magnetic resonance spectrum to be expected.

In Chapter III, the NMR spectrometer and electromagnet used, as well as the nuclear induction method, are described. A description of the sample is also given. An account of the steps taken to obtain the spectra is the subject of Chapter IV, while Chapter V contains the data analysis and the experimental results.

The final chapter, Chapter VI, gives a discussion of these results, as well as a description of the calculations performed in an attempt to reconcile the experimental results with those predicted by theory. The final chapter also tells why we are confident in the experimental results and in their explanation, and includes a brief word as to what might be expected at the low temperatures of interest described above.

CHAPTER II

THEORY

1) Development of the Hamiltonian for the Vanadium Nucleus

We now introduce and develop the general Hamiltonian H_V of the system. The system comprises the V^{5+} ions in the $DyVO_4$ crystal, when placed in an externally applied static homogeneous magnetic field $\vec{H}_0$.

In general the Hamiltonian for the V^{5+} nuclei which are embedded in the paramagnetic salt $DyVO_4$, subjected to an external field, may be written as a sum of three terms:

$$H_V = H_Z + H_M + H_Q$$

where H_Z is the Zeeman term, H_M the magnetic ion interaction term, and H_Q the electric quadrupole interaction contribution.

H_Z, the Zeeman interaction, splits the energy levels into $2I+1 = 8$ components associated with the 8 values of the quantum number m describing the spacial quantization of the spin in the magnetic field. This Zeeman contribution may be written as:

$$H_Z = -g_N \beta_N \vec{H} \cdot \vec{I} \ ,$$

$$(\text{or} \quad H_Z = -\gamma \hbar \vec{H} \cdot \vec{I} = -\gamma \hbar H I_Z) \ ,$$

where g_N and β_N are the nuclear splitting or g-factor and the nuclear magneton, respectively. $\vec{H}$ is the external field, and I the nuclear spin, while γ is the gyromagnetic ratio. This

Zeeman effect separates the 8-fold degenerate state into 8 levels equidistant in energy, as shown in Fig. II. The conditions for a NMR transition are that $\Delta m = \pm 1$, and the r-f frequency is related to the energy difference by $\Delta E = h\nu$. The result of the selection rule is that the 7 observable NMR transitions are at the same frequency and experimentally only one single resonance is observed.

H_M, the interaction of the magnetic ions with the nucleus, can be expressed in the form:

$$H_{M_i} = \sum_j \langle S_j \rangle \cdot A_{ji} \cdot I_i, \quad (8)$$

where $\langle S_j \rangle$ is the thermally averaged value of the electronic spin on the j'th Dy^{3+} ion and A_{ij} is the interaction tensor. The latter is usually the sum of two terms. One is the so-called transferred hyperfine (TH) interaction, and the other is the classical dipolar interaction. The thermally averaged spin can be related to the magnetization of the sample. Then H_M can be written in the form:

$$H_M = -g_N \beta_N \vec{H} \cdot \vec{C} \cdot \vec{I} \quad (8),$$

where the so-called field shift tensor $\vec{C}$ is field-independent.

The third term to be included in the Hamiltonian is the quadrupole interaction term, H_Q. The energy of interaction is a function of the orientation of the nucleus with respect to its electrostatic environment, and therefore of the magnetic quantum number m describing this orientation. The effect of the quadrupole interaction (see Fig. II) is to displace the $2I+1$ energy levels, and the $2I=7$ intervals between the successive energy levels are now no longer equal. If, there-

Fig. II

Illustration of the various splittings of the 8-fold ground level of the ^{51}V nucleus. The four cases are those of zero-field, Zeeman splitting, first-order quadrupole interaction splitting, and the second-order quadrupole interaction splitting. The latter has been included only for the levels denoted by $m=\frac{1}{2}$ and $m=-\frac{1}{2}$, as the second-order splitting affects only the $m_{\frac{1}{2}} \leftrightarrow m_{-\frac{1}{2}}$ transition in the NMR spectrum.

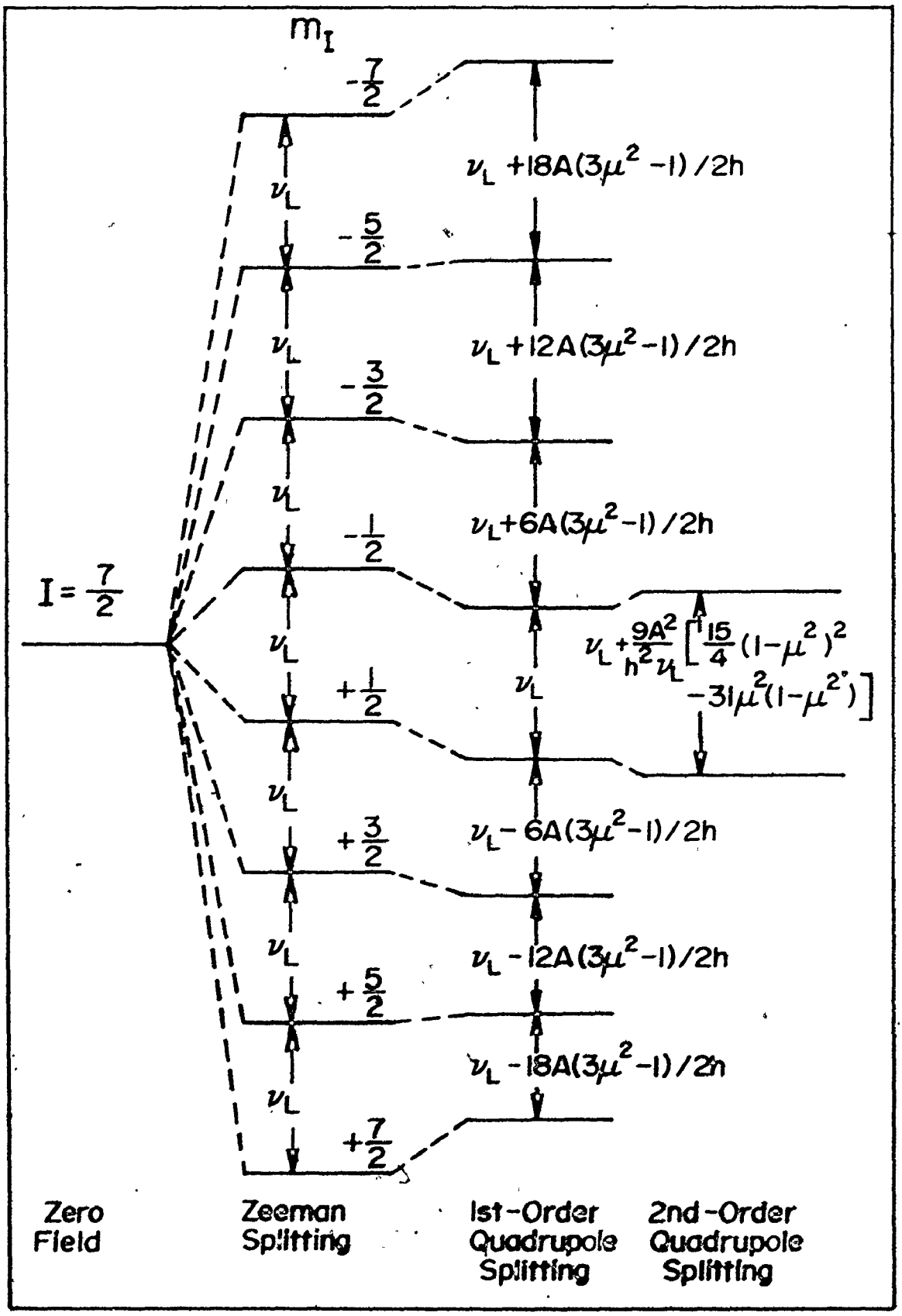
m_I
$-\frac{7}{2}$
$-\frac{5}{2}$
$-\frac{3}{2}$
$-\frac{1}{2}$
$+\frac{1}{2}$
$+\frac{3}{2}$
$+\frac{5}{2}$
$+\frac{7}{2}$
$I=\frac{7}{2}$
ν_L
$\nu_L + 18A(3\mu^2-1)/2h$
$\nu_L + 12A(3\mu^2-1)/2h$
$\nu_L + 6A(3\mu^2-1)/2h$
$\nu_L - 6A(3\mu^2-1)/2h$
$\nu_L - 12A(3\mu^2-1)/2h$
$\nu_L - 18A(3\mu^2-1)/2h$
$\nu_L + \frac{9A^2}{h^2\nu_L}\left[\frac{15}{4}(1-\mu^2)^2 - 31\mu^2(1-\mu^2)\right]$
Zero Field
Zeeman Splitting
1st-Order Quadrupole Splitting
2nd-Order Quadrupole Splitting

fore, we have a single crystal containing nuclei at equivalent lattice sites, the resonance spectrum is split into 7 component lines, approximately symmetrically displaced on either side of the position the line would take in absence of the quadrupole interaction. In first order, it will be seen that, m being half-integral, the $m_{\frac{1}{2}} \leftrightarrow m_{-\frac{1}{2}}$ transition gives a component line in this central position. However, if the quadrupole interaction is strong enough to include a second-order term, it is found that even this component ($m_{\frac{1}{2}} \leftrightarrow m_{-\frac{1}{2}}$) is shifted, and has angular dependence. In these experiments, only first and second order quadrupole effects are visibly of importance.

Any standard text on the phenomenon of nuclear magnetic resonance includes a formal derivation of the quadrupolar interaction Hamiltonian H_Q [9], and it serves no purpose to quote it here. It can be shown, however, that in the principal axes coordinate system we have that the quadrupolar part of H_V is, in general, given by:

$$H_Q = A[3I_Z^2 - I(I+1) + \tfrac{1}{2}\eta(I_+^2 + I_-^2)] \quad (8),$$

$$A = \frac{e^2qQ}{4I(2I-1)},$$

$$eq = V_{ZZ},$$

$$\eta = \frac{V_{XX} - V_{YY}}{V_{ZZ}} \qquad 0 \leq \eta \leq 1,$$

$$|V_{ZZ}| \geq |V_{YY}| \geq |V_{XX}|,$$

$$I_\pm = I_X \pm iI_Y.$$

eQ is the nuclear quadrupole moment and $V_{ij} = \frac{\partial^2 V}{\partial X_i \partial X_j}, (X_i, X_j = X, Y, Z)$,

are the components of the electric field gradient tensor in the principal axes system. The most general field gradient is therefore specified by the orientation of the principal axes of the field gradient tensor and by the two parameters q and η. If the field gradient is axially symmetric, then $V_{XX}=V_{YY}$, and $\eta=0$. The parameter η is in fact termed the "asymmetry parameter" and measures the departure of the field gradient from cylindrical symmetry. From the symmetry of the $DyVO_4$ crystal and from the fact that each vanadium has a 4-fold axis of symmetry, $\eta=0$.

Finally, therefore, we may write that the Hamiltonian for our system, in the principal axes coordinate system, is:

$$H = -g_N\beta_N[H_X(1+C_{XX})I_X + H_Y(1+C_{YY})I_Y + H_Z(1+C_{ZZ})I_Z]$$

$$+ A[3I_Z^2 - I(I+1)], \quad C_{XX} = C_{YY}.$$

The eight energy levels may be readily obtained by a numerical diagonalization of the 8x8 matrix that results for $I = \frac{7}{2}$. The differences between the energy levels may then be fitted to the data by a least squares procedure to obtain the parameters in the Hamiltonian, namely C_{XX}, C_{ZZ}, and A. It is to be noted that in the above expression for the Hamiltonian, $C_{XX}I_X$ denotes an extra contribution to the field at the vanadium site due to factors which scale with the magnetization. It would therefore be expected that the parameters C_{XX} and C_{ZZ} should scale with the magnetization in the corresponding directions.

ii) Description of the Angular Dependence of the NMR Spectrum Expected from the Quadrupole Interaction

Once again, any well-known NMR text (such as The Principles of Nuclear Magnetism, by A. Abragam) will show how, using second-order perturbation theory, that the first three contributions to the energy levels are given by:

$$E_m^{(0)} = \mathcal{H} H_m = -h\nu_L m,$$

$$E_m^{(1)} = \tfrac{1}{4}h\nu_Q(3\mu^2-1)(m^2-\tfrac{1}{3}a),$$

$$E_m^{(2)} = -h\left(\frac{\nu_Q^2}{12\nu_L}\right)m\left[\tfrac{3}{2}\mu^2(1-\mu^2)(8m^2-4a+1) + \tfrac{3}{8}(1-\mu^2)^2 \times (-2m^2+2a-1)\right] \quad (10),$$

where $a = I(I+1)$, $\mu = \cos\theta$, $\nu_L = \frac{\gamma H}{2\pi}$ = Larmor frequency, and, for brevity, the frequency $\nu_Q = \frac{3e^2qQ}{2Ih(2I-1)}$. It can then be shown that the first-order change in the frequency associated with any transition is given by:

$$\nu_m^{(1)} = \frac{E_{m-1}^{(1)} - E_m^{(1)}}{h} = \nu_Q(m-\tfrac{1}{2})\left(\frac{3\mu^2-1}{2}\right) \quad (9),$$

which vanishes for $m = \frac{1}{2}$.

The second-order shift $\nu_m^{(2)} = \frac{E_{m-1}^{(2)} - E_m^{(2)}}{h}$, for the central NMR signal, is given by:

$$\nu_{\frac{1}{2}}^{(2)} = -\frac{\nu_Q^2}{16\nu_L}(a-\tfrac{3}{4})(1-\mu^2)(9\mu^2-1) \quad (9).$$

It is worth pointing out that $E_m^{(2)}$ is an odd function of m. Therefore we have that $\nu_m^{(2)} = \frac{1}{h}(E_{m-1}^{(2)} - E_m^{(2)})$, and

$\nu_{-m}^{(2)} = \frac{1}{h}(E_{-m}^{(2)} - E_{-(m-1)}^{(2)})$ are equal and so $\Delta\nu = \nu_m^{(2)} - \nu_{-m}^{(2)} = 0$.

Therefore the first-order formula $\Delta\nu = \nu_Q(m-\frac{1}{2})\frac{(3\mu^2-1)}{2}$ expressing the frequency separation, between any 2 satellite signals $(m-1)\leftrightarrow m$ and $-m\leftrightarrow-(m-1)$, is also correct in second-order.

For the case of vanadium, with $I = \frac{7}{2}$, we have

$\nu_Q = \frac{3e^2qQ}{h2I(2I-1)} = \frac{e^2qQ}{14h}$, while $A = \frac{e^2qQ}{4I(2I-1)} = \frac{e^2qQ}{14x6} = \frac{h\nu_Q}{6}$.

Thus, for vanadium, the first-order change in frequency is given by:

$$\nu_m^{(1)} = \frac{3A}{h}(m-\tfrac{1}{2})(3\mu^2-1), \quad \mu = \cos\theta.$$

For any given satellite the maximum shift magnitudes occur for $\theta = \frac{n\pi}{2}$, n = 0,1,2..., and the zero for θ=54.7°. Although any 2 inequivalent angles would have sufficed for investigation in the experiments performed, the two special orientations corresponding to θ=0°(c-axis $\parallel \vec{H}o$), and $\theta=\frac{\pi}{2}$ (c-axis $\perp \vec{H}o$) were the easiest and most accurately studied, as the satellites are separated by equal intervals of 6A and 3A, respectively.

CHAPTER III

EXPERIMENTAL APPARATUS AND TECHNIQUE

1) Description of Varian NMR Spectrometer and Cross-Coil Induction Method

The instrument used for inducing and observing the NMR signals from our sample was a Model V-4200B Wide-Line NMR Spectrometer manufactured by Varian Associates of Palo Alto, California. A block diagram of the spectrometer is given in Fig. III.

The spectrometer comes with crossed-coil probes, with frequency ranges of 2-4 MHz, 4-8 MHz, and 8-16 MHz. In addition to holding the sample, the probe contains a pair of sweep coils (modulation coils) for producing periodic variations in the external field H_0, a transmitter coil for producing the H_1 rotating field, a receiver coil for detecting the NMR signal, and two sets of paddles for adjusting the leakage signal between the transmitter and receiver coils. The phase of the leakage determines the mode of operation, dispersion or absorption.

The technique used for inducing and detecting the signals is the "cross-coil" method, in which a radio-frequency transmitter generates an oscillating magnetic field of amplitude $2H_1$ in the transmitter coil which contains the sample under investigation. The receiver coil axis is positioned perpendicular to the transmitter coil and the static magnetic field. For

Fig. III

Block diagram of the Varian Model V-4200B Wide-Line NMR Spectrometer. The diagram shows the basic components of the spectrometer, their interrelation, and the process of the transmission, reception, and final display of the NMR signal.

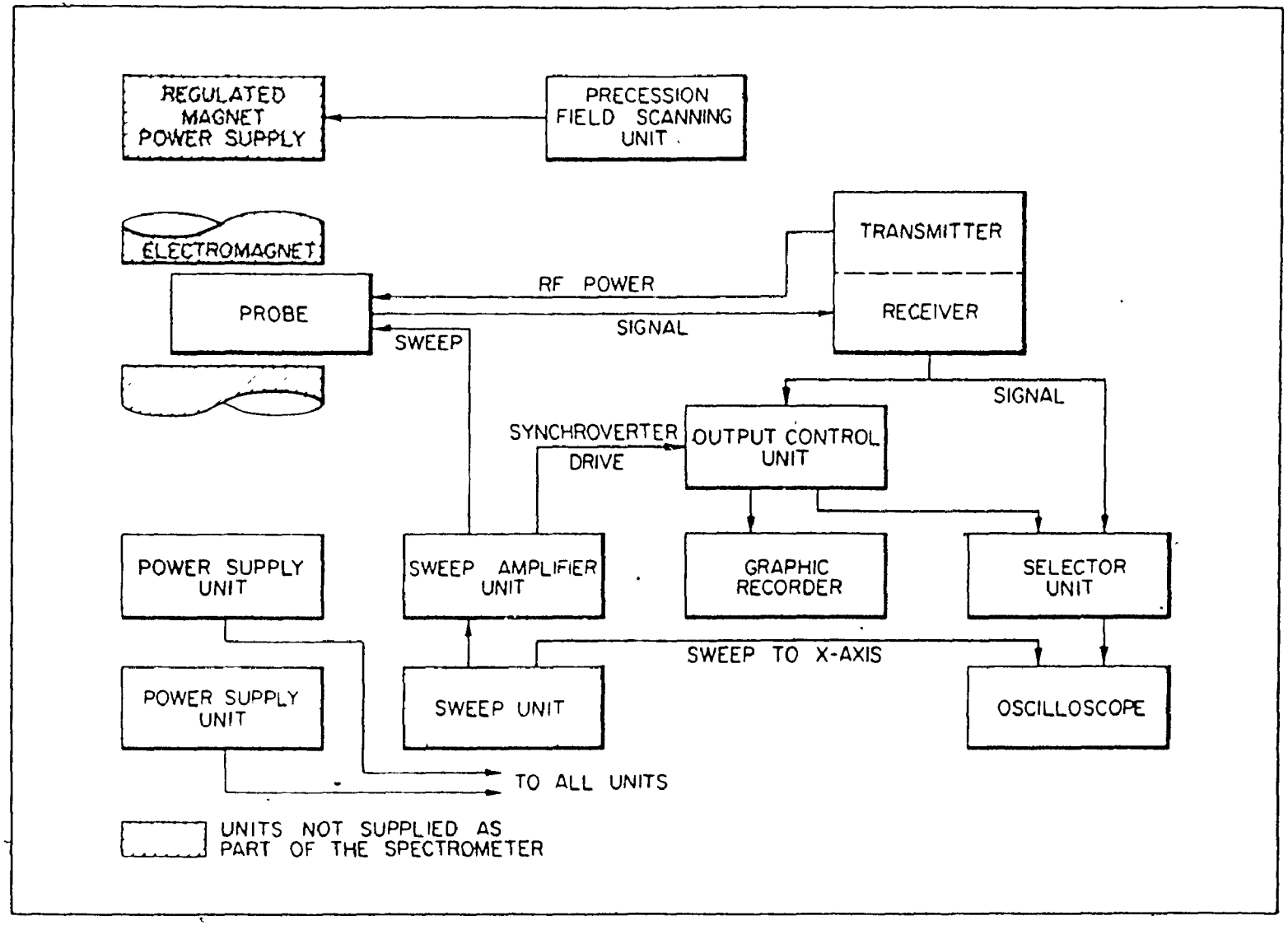
REGULATED MAGNET POWER SUPPLY
PRECESSION FIELD SCANNING UNIT
ELECTROMAGNET
TRANSMITTER
PROBE
RF POWER
RECEIVER
SIGNAL
SWEEP
SIGNAL
SYNCHROVERTER DRIVE
OUTPUT CONTROL UNIT
POWER SUPPLY UNIT
SWEEP AMPLIFIER UNIT
GRAPHIC RECORDER
SELECTOR UNIT
SWEEP TO X-AXIS
POWER SUPPLY UNIT
SWEEP UNIT
OSCILLOSCOPE
TO ALL UNITS
UNITS NOT SUPPLIED AS PART OF THE SPECTROMETER

inducing transitions $\Delta m = \pm 1$ it is also necessary that the transmitter coil axis be perpendicular to the static magnetizing field.

The frequency of the r-f transmitter was set at a particular value, and the expected value of the resonant magnetizing field H_o for vanadium was also set, according to:

$$H_r = \frac{\nu o}{\gamma}$$

where γ is the gyromagnetic ratio for vanadium nuclei. As the value of H_o is swept through H_r, a signal voltage is induced in the receiver coil of the probe. This signal appears as a modulation of the magnetic coupling or so-called "leakage" between the transmitter and the receiver coils. In order to display the resonance signal, (absorption or dispersion), the 'steady'field H_o is sinusoidally modulated at a low audio-frequency with an amplitude of a few oersteds. When H_o is close to the resonant value, the field is swept through the resonant condition, producing an audio-frequency amplitude modulation of the r-f carrier. The modulated r-f signal is amplified and demodulated to recover the audio-frequency signal by an amplifier-detector, (the receiver), which is tuned to the same frequency as the transmitter. This demodulated audio-signal is then delivered both to an oscilloscope for visual observation, as well as to a phase-sensitive detector and chart recorder.

The above-mentioned magnetic leakage signal, from the transmitter coil to the receiver coil, must be critically adjusted to obtain optimum spectrometer operation. Both the

magnitude and the phase angle of this leakage must be controlled. The cross-coil configuration constitutes an effective mechanical radio-frequency bridge. The spectrometer is operated with this bridge slightly unbalanced, for reasons of detector sensitivity. By unbalancing the leakage signal with respect to amplitude, one obtains the absorption mode. Unbalancing the leakage with respect to phase, however, yields a signal in the dispersion mode. The distinction between absorption and dispersion can be explained as follows. Suppose the magnetizing field H_o is parallel to the Z-axis and the r-f field is parallel to the X-axis. In this model, the magnetization vector M_o is projected onto the X-Y plane as a vector M_{XY} which has 2 components; M_X along the X-axis and M_Y along the Y-axis. When the leakage is in phase with the M_X vector, the spectrometer is said to be operating in the u-mode or dispersion mode, associated with the real in-phase part χ' of the complex magnetic susceptibility $\chi=\chi'+i\chi''$. When the leakage is in-phase with the M_y vector, operation is in the v-mode or absorption mode, which is associated with the out-of-phase imaginary part χ'' of the susceptibility. Although it is possible to obtain a mixture of these two modes, it is usual to work either in one or the other.

The undesired leakage component is cancelled while the other is controlled, this being done by means of a set of paddles for each of the modes — the red or v-mode paddles and the blue or u-mode paddles. Each of the red paddles is a highly conducting circular disc attached to the end of a threaded plastic rod which can be moved in and out of the transmitter

coil field. The blue paddles are similar in construction except that the disc is replaced by a ring of resistive material.

After the sample has been inserted and the approximate r-f level has been set, the paddles are adjusted for minimum leakage. First one fine paddle is adjusted for minimum detector current, then the other. This is repeated until the meter reads approximately zero. After this null has been reached, about 10 to 20 μV of leakage is introduced in the desired mode with the appropriate paddle.

It is, of course, desirable to operate the transmitter at high power levels to obtain a good signal-to-noise ratio, but when operating on v-mode or absorption mode this value is limited by sample saturation. The optimum settings of both the r-f power and the modulation field amplitude have to be determined experimentally. Usually excess of both are used to find the signals. They are then reduced until an optimum compromise between signal-to-noise ratio and line width is reached.

Before actual operation of the equipment, and measurement of the signals is performed, both the spectrometer and the associated electromagnet system are allowed to reach thermal equilibrium. This usually requires a minimum of 3/4 hour in order to reduce r-f frequency and magnetic field drifts.

ii) Size and Mounting of Sample in Probe

The crystals of $DyVO_4$ contained in the sample used in these experiments were grown by Mr. Fred Long in 1972, using a flux method.[12] The crystals chosen were the largest ones obtainable having at the same time the property that they

resemble as closely as possible a rectangular parallelepiped, and that they all be of approximately the same dimensions.

A total of nine crystals in all were mounted on a smooth flat thin slab of potassium chloride, in three layers of three each. The crystals were carefully aligned and fitted together in a parallel manner so that their long or c-axes were parallel. The result hopefully resembles a single crystal of $DyVO_4$, of dimensions 0.65 cm (c-direction) by 0.6cm by 0.35cm. The cleaved potassium chloride crystal was used as a mount since it formed a very flat surface, and would give rise to no interfering NMR signals. The $DyVO_4$ crystals were mounted together with G.E. 7031 cement.

The sample so formed was then mounted (once more with G.E. 7031 cement) onto the end of a long cylindrical nylon rod support, in such a way that the a-c plane of the crystal was perpendicular to the rod axis. The other end of the nylon rod was threaded so that the vertical position of the sample could be accurately adjusted. The rod was also fitted with an angular scale to measure the rotation of the sample. A diagram of the dewar-support assembly is shown in Fig. IV.

The sample height in the dewar was adjusted so that it was as centrally placed as possible in the receiver coil of the Varian probe.

Fig. IV

Schematic cross-sectional view of the sample support and dewar assembly, as mounted in the Varian probe. The 'static' homogeneous field $\vec{H}_0$ direction, perpendicular to both the transmitter and receiver coils, is also shown.

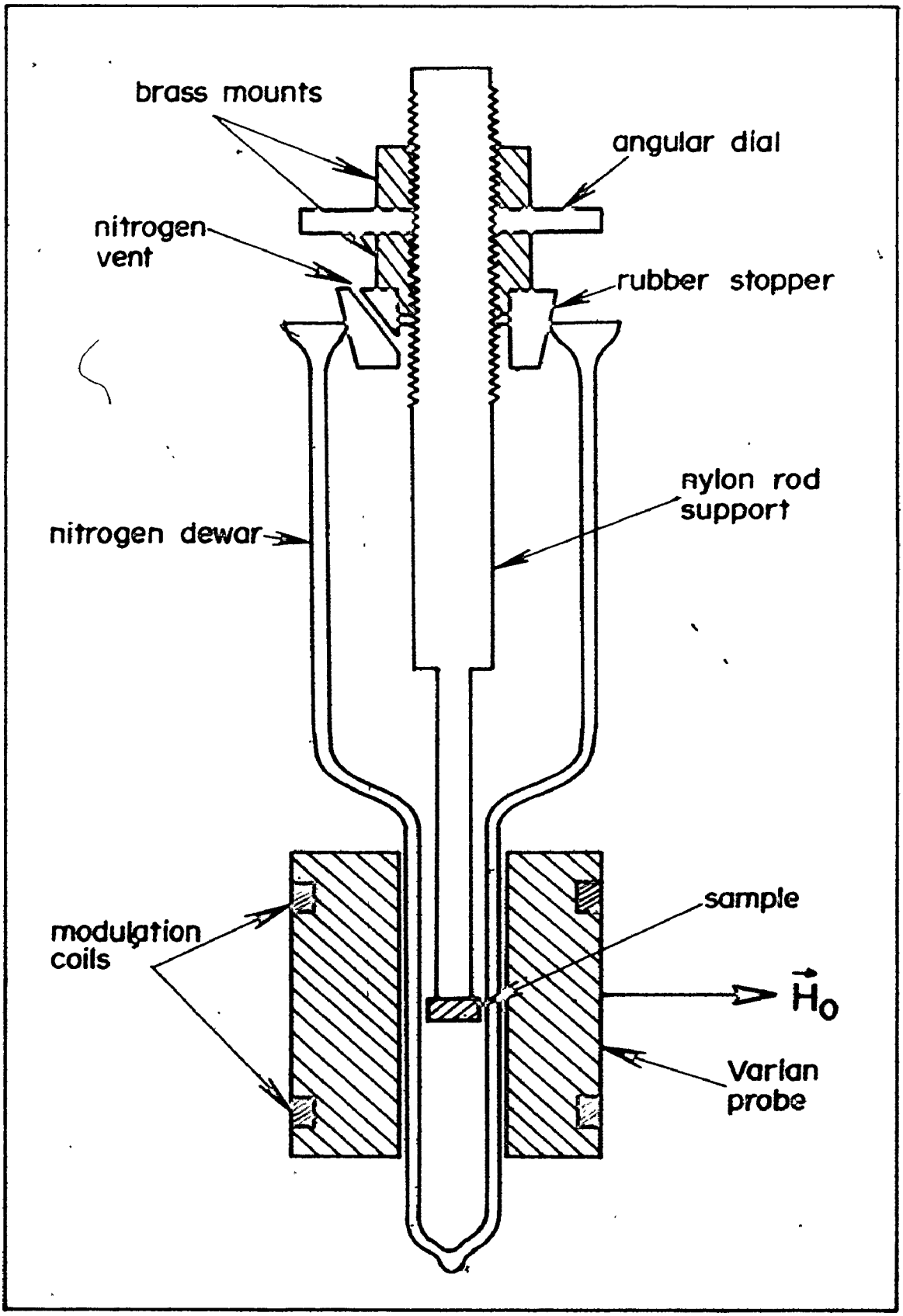
brass mounts
angular dial
nitrogen vent
rubber stopper
nylon rod support
nitrogen dewar
modulation coils
sample
$\vec{H}_0$
Varian probe

CHAPTER IV

DATA ACQUISITION

1) Spectrometer Optimization

Two r-f frequencies were used to obtain data, nominally 8 and 16 MHz. Since, for a 10kOe field, a frequency of 11.193 MHz is required for resonance, a field of H_o = 14.295 kOe was set for 16 MHz and H_o = 7.147 kOe was set for 8 MHz.

Two temperatures were investigated, room temperature (taken to be T = 292°K), and liquid nitrogen temperature (T = 77°K). Good quality data were found to be obtainable at T = 292°K for both r-f frequencies. Data were only obtainable at T = 77°K, for the 16 MHz frequency, as at the lower frequency the signal-to-noise ratio was too poor to allow any sensible readings to be taken. The extra noise at T = 77°K was due to the bubbling of the liquid nitrogen in the dewar.

For each temperature and/or frequency investigated, the probe used was balanced for the absorption mode. With a sweep range of 2.5 kOe, and a sweep time of 50 minutes, a first trace was run of the $DyVO_4$ spectrum with the c-axis parallel to $\vec{H}_o$ where the greatest satellite separation was expected. After this, optimum conditions of modulation amplitude and r-f power were set by trial and error.

ii) Angular Range

Due to the anisotropy of the magnetic susceptibility, it is necessary to record the data for at least two non-symmetry-related directions. The best choice would be $\vec{H}_o$ parallel to the c-axis, called $\theta=0$, and $\vec{H}_o$ perpendicular to $\vec{c}$, called $\theta=\pi/2$. A full angular range of 90° was recorded, in steps of 10° between 0° and 40°, steps of 5° between 40° and 70°, and then 10° between 70° and 90°. The 5° steps in the mid-range were taken in order to facilitate identification and labelling of the satellites in that range where they crossed over and were superimposed. This was not an easy task even with the traces of better signal-to-noise ratio.

iii) Determination of Field and Frequency

All NMR traces were recorded with a fixed frequency and the magnetic field was swept at a constant rate. The chart recorder also advanced at a constant rate so that distance along the chart recorder paper could be equated to changes in magnetic field.

It should be pointed out at this stage that since a field sweep range of 2.5 kOe was used (in order to include all satellites at their maximum separation), all traces included an NMR resonance from the aluminum nuclei in the probe. This reference served as a convenient field reference (for a given frequency) which could be used as a standard against which to refer all the vanadium resonance shifts. Of course, the aluminum signal from the metallic probe is a Knight-shifted signal from that expected from an aqueous solution of aluminum ions. A solution of $Al(NO_3)^3$ was therefore used to measure

the Knight shift for a given H_o, as well as to measure the field dependence, if any, of the Knight shift. It was found that the Knight shift was a constant percentage of H_o, as expected, (see Fig. V). The value of 0.154±0.031% agreed well with the value of 0.162 as quoted in L. F. Drain's (11) review on NMR in metals.

iv). Susceptibility and Magnetization Data

Since, as discussed above, it is expected that the components of the field shift tensor $\vec{C}$ should scale with the corresponding components of the magnetization $\vec{M}$, we need to have data for the magnetization, at both temperatures of interest in the two perpendicular directions $\Theta=0$ and $\Theta=\pi/2$. These values, for T = 77°K and T = 292°K, were measured by Dr. Carl Stager, using a Princeton Applied Research Vibrating Sample Magnetometer. It will also be found later that these values are necessary for calculating demagnetizing and dipole fields.

Fig. 1

Graph illustrating the field dependence of the Knight shift of the probe aluminum signal from an aluminum ion aqueous solution signal.

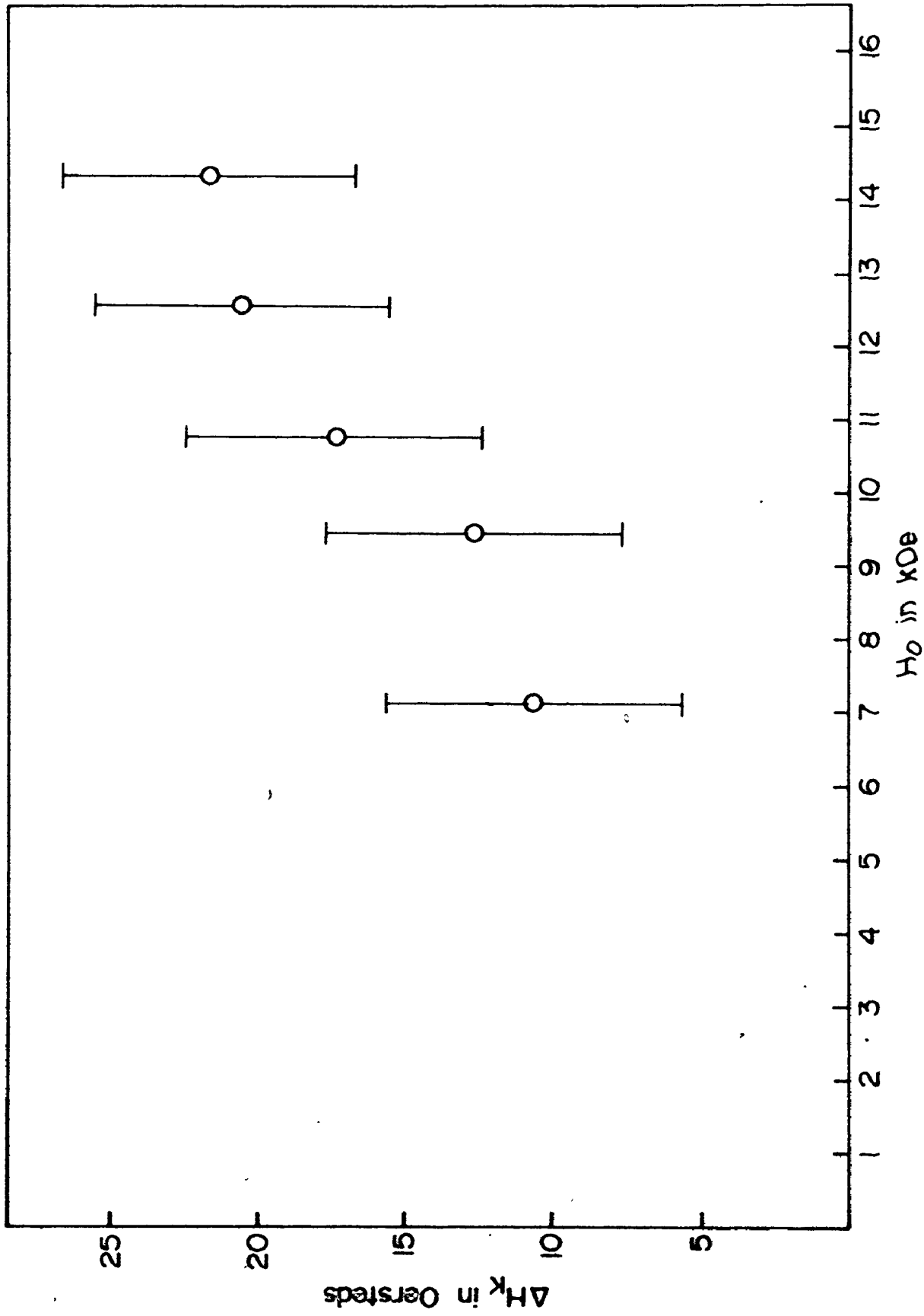
ΔHK in Oersteds
25
20
15
10
5
1
2
3
4
5
6
7
8
9
10
11
12
13
14
15
16
Ho in kOe

CHAPTER V

DATA ANALYSIS AND RESULTS

As expected, the NMR field traces for the vanadium nuclei showed a central component accompanied by six satellite peaks which, for =0, were separated by equal field intervals and were approximately symmetrically displaced from the central component, (see Fig. VII). The angular variation of the satellite and central components is shown in Figs. VIII and IX. It is seen that, overall, the results are at least qualitatively in keeping with what is expected according to theory, and a second-order angular dependence of the central component and its shift is also observed.

As mentioned above, both the central component and the six satellites, for all the NMR traces obtained, were able to be referred to the probe's aluminum signal. Using the measured Knight shift for the aluminum signal from the probe relative to that from an aqueous solution, the positions of all vanadium signals could be referred to the known field position of the Al_{aq} signal (for a given r-f frequency used). In this fashion, the field positions of all the vanadium peaks for all runs were determined.

It must be noted that an important factor which had to be included in the analysis of the traces was the calibration of the sweep speed. That is, the true rate of change of the

Fig. VI

Example of a typical ^{51}V NMR trace. The trace is taken at the orientation $\theta=0$ at $T = 292°K$. The scale of the diagram is such that there are approximately 288 Oe between neighbouring satellites.

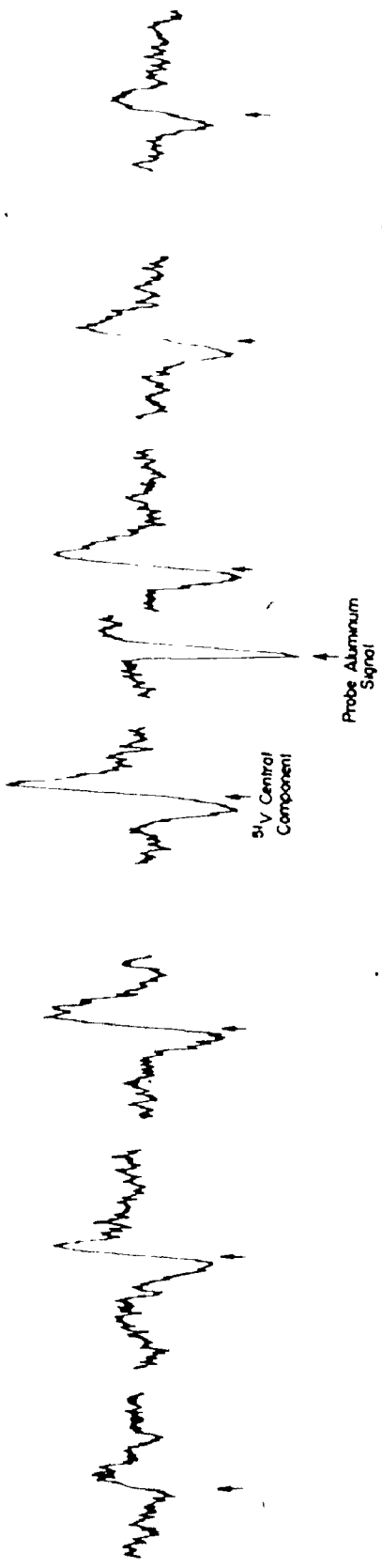
Probe Aluminum Signal
^{51}V Central Component

magnetic field had to be measured. Although the instrument has a calibrated sweep the accuracy was not sufficient for these experiments.

The calibration was performed in the following manner. The sweep range was set at 2.5 kOe, the value used during the experiment, and the 'steady' homogeneous field H_o initially set at the calculated resonant value for an aqueous solution of vanadium ions, i.e. H_o = 14.295 kOe. The sweep range percent dial was then successively set at intervals of 10% from -50% to +50% of the range. The r-f frequency was altered to measure the field at each setting using the ^{35}Cl resonance from a solution of LiCl. This frequency was recorded and the corresponding expected chlorine resonance field value calculated. At the same time, of course, the sweep range percent value yielded a different figure. The measured minus the instrument data were plotted and are shown in Fig. VII. Within reasonable error limits the plot is a straight line of slope 1.00699. This indicated that in fact 50.350 Oe/min. were being swept, compared with the nominal instrument value of 50.0 Oe/min. The difference is small but significant.

In the calibration plot, the field error represented by the intercept $(\Delta H)_o$ is of no interest as the use of the internal Al standard removes all field errors that are independent of the position in the sweep range. The difference ΔH may be represented by $\Delta H = (\Delta H)_o + Kf$, where f is a measure of the percentage of the sweep range and K is the slope of the graph. If the manufacturer's calibration had been perfectly accurate, both $(\Delta H)_o$ and K would be zero.

Figs. VII (a) and (b)

Field sweep rate calibration plots. Fig. VII (a) is at the higher field of H_0=14.295 kOe, while Fig. VII(b) is for the lower field of H_0=7.147 kOe.

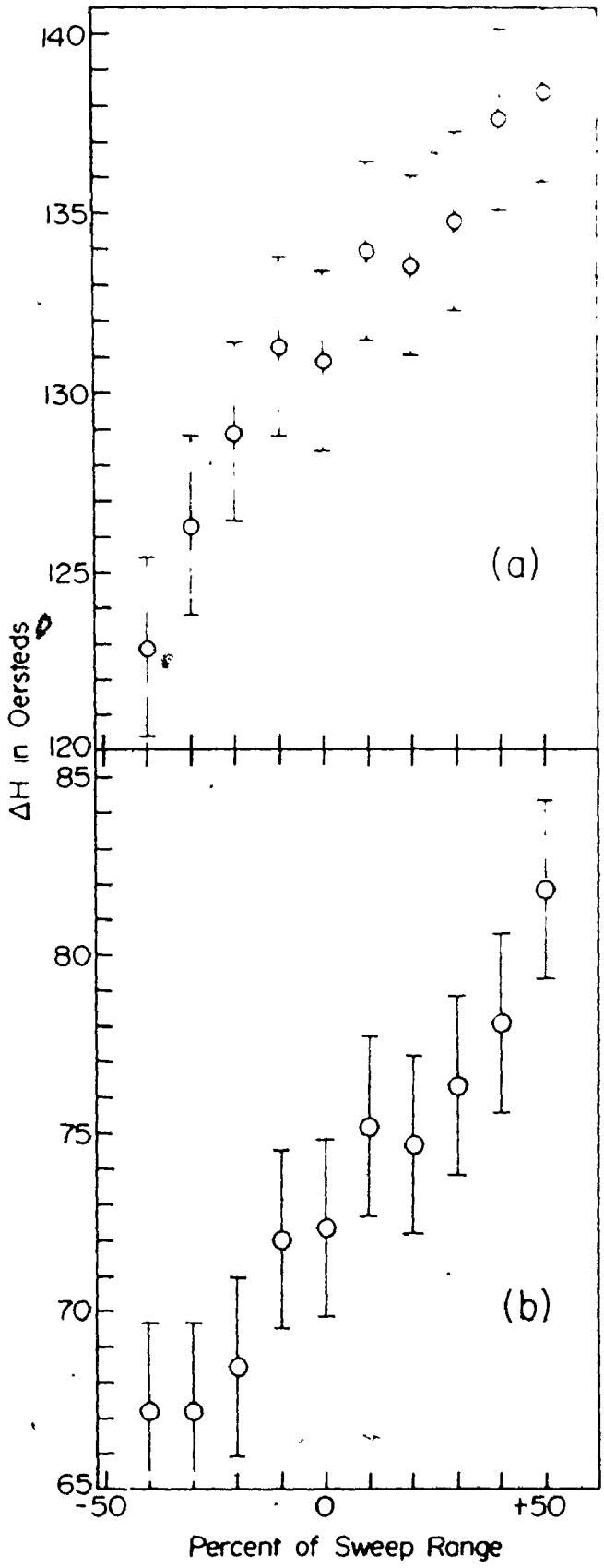
140
135
130
125
120
(a)
85
80
75
70
65
(b)
ΔH in Oersteds
-50
0
+50
Percent of Sweep Range

The same calibration procedure was carried out at H_o = 7.147 kOe, i.e. for 8 MHz. In this case, using the Li signal in the same LiCl solution, it was found that the best fit yielded a result of 50.318 Oe/min., and therefore a shift multiplication factor of 1.00635. An average correction factor was therefore calculated as 1.0066 ± 0.0017, resulting from an average field sweep of 50.334 ± 0.086 Oe/min.

For the room temperature experiments, a reasonably good signal-to-noise ratio was obtained at both frequencies used, and the majority of satellites were clearly visible and identifiable in the angular ranges of 0° to 45°, and 70° to 90°. This was not the case, however, for all the satellites within the angular range of 45° to 70°, wherein the satellites 'cross over' and overlap. In the data, only the certainly identifiable satellites were included for all angles.

For the experiments performed at liquid nitrogen temperature, i.e. 77°K, the signal-to-noise ratio was markedly reduced, due mainly to the mechanical vibrations experienced from the bubbling of the nitrogen in the dewar. However, although no data of any reasonable quality were obtainable at the lower frequency of 8 MHz quite good data were available at 16 MHz, the higher frequency.

It should be noted that the frequency generator had a tendency to drift, that is, to decrease with time. The rate of decrease of frequency with time was measured and found to be about $94.4S^{-1}$/min, at the time the data were taken at MHz, and $21.9S^{-1}$/min at the time the data were taken at 16 MHz.

These decreases corresponded to an average loss of 0.0047 MHz per scan at the lower frequency, and of 0.0012 MHz per scan at the higher frequency. This fact was therefore taken into account when assigning a frequency to a given scan, that is, to a given angle θ under investigation.

The data, that is, the r-f frequency, the absolute field positions of the satellites and their label number, as well as the angle θ, were fitted, via a least squares program (developed by E. R. Cowley).

to the Hamiltonian given in Chapter II, namely

$$H = -g_N\beta_N[H_X(1+C_{XX})I_X + H_Y(1+C_{YY})I_Y + H_Z(1+C_{ZZ})I_Z] + A[3I_Z^2 - I(I+1)], \quad C_{XX} = C_{YY}.$$

The program essentially sets up an Hermitian matrix whose elements are functions of C_{XX}, C_{YY}, C_{ZZ}, H_X, H_Y, H_Z, and A. This matrix is then diagonalized completely, the eigenvalues determined and the difference of the eigenvalues are fitted to the experimental data. The procedure gives "best fit" values of C_{XX}, C_{ZZ}, and A, together with their standard errors, for the two temperatures. A non-linear least squares procedure requires estimated values of the parameters. For C_{XX} and C_{ZZ} these were chosen to be 1×10^{-3}. The value of A was estimated initially from the maximum separation of satellites when $\theta=0$.

The program tabulates the predicted and experimentally-observed field shifts of all seven peaks at all angles investigated, as well as the differences between the two. The predicted and experimentally-observed field shifts are plotted

versus θ for all NMR lines in Figs. VIII and IX.

In this work, we are not only interested in the quadrupolar angular dependence of the vanadium peak shifts, but also with the temperature dependence of C_{XX} and C_{ZZ} along the symmetry directions $\vec{a}$ and $\vec{c}$, respectively, of the $DyVO_4$ crystal, as well as the temperature dependence of the quadrupole coupling factor A. The resulting values for these quantities are given in Table 1, together with the magnetization data obtained for the two temperatures and the two orientations of interest in these experiments.

Fig. VIII

Angular dependence of the field shifts of the central and satellite components of the ^{51}V spectrum in $DyVO_4$, for $\nu_Q = 8$ MHz. The shifts are referenced to the expected position for a vanadium aqueous solution. The solid lines are calculated from the parameters obtained from the least squares fit to the data for T=292°K. The circles are the experimental points for T=292°K.

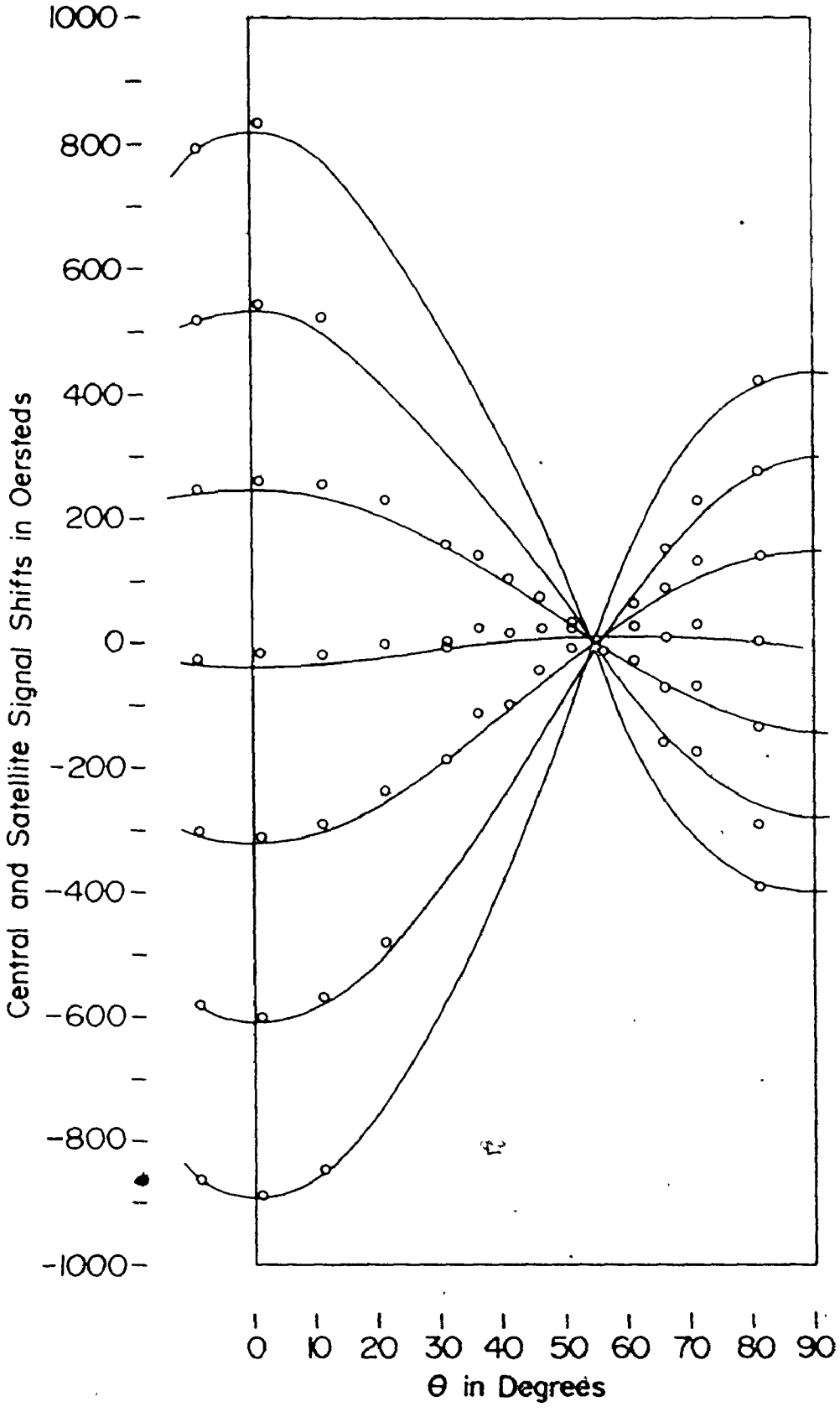
1000
800
600
400
200
0
-200
-400
-600
-800
-1000
Central and Satellite Signal Shifts in Oersteds
0
10
20
30
40
50
60
70
80
90
θ in Degrees

Fig. IX

Angular dependence of the field shifts of the central and satellite components of the ^{51}V spectrum in $DyVO_4$, for ν_o=16 MHz. The solid lines are calculated from the parameters obtained from the least squares fit to the data for T=292°K, while the circles are the experimental points for T=292°K. The dashed curves and the triangles are the least squares predicted curves and the experimental points, respectively, for T=77°K.

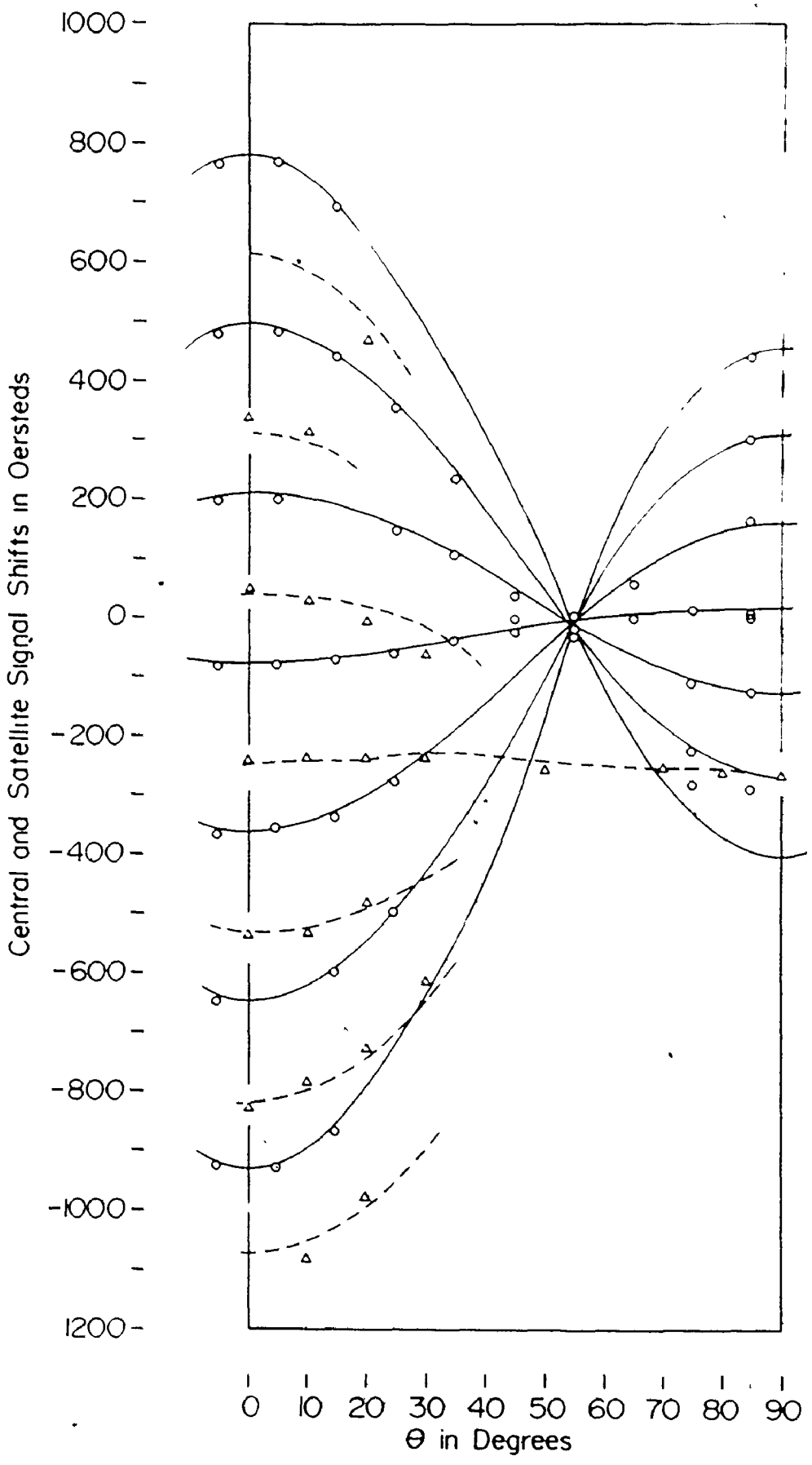
1000
800
600
400
200
0
-200
-400
-600
-800
-1000
1200
Central and Satellite Signal Shifts in Oersteds
0
10
20
30
40
50
60
70
80
90
Θ in Degrees

Table 1

The table gives the values of the parameters C_{XX}, C_{ZZ}, and A for the 2 temperatures investigated. The measured values of the magnetization in the directions $\theta=0$ and $\theta=\pi/2$ are also included. The ratios of the values of M at the 2 temperatures are given for $\theta=0$ and $\theta=\pi/2$, and are compared with the ratios of C_{ZZ} and C_{XX}, respectively, for the same 2 temperatures.

	T = 292°K		T = 77°K	
	$\vec{H} \parallel \vec{c}$	$\vec{H} \perp \vec{c}$	$\vec{H} \parallel \vec{c}$	$\vec{H} \perp \vec{c}$
C_{XX}		- 0.0016 ± 0.0003		0.0182 ± 0.0008
C_{ZZ}	0.0054 ± 0.0002		0.0173 ± 0.0004	
A		- 0.0479 ± 0.0002		- 0.0495 ± 0.0004
M	12.351	15.997	18.526	63.988
	±0.494 emu/cc	±1.120 emu/cc	±0.741 emu/cc	±2.560 emu/cc
	$\frac{M(292)}{M(77)} = 0.667 \pm 0.073$	$\frac{M(292)}{M(77)} = 0.250 \pm 0.028$	$\frac{C_{ZZ}(292)}{C_{ZZ}(77)} = 0.319 \pm 0.020$	$\frac{C_{XX}(292)}{C_{XX}(77)} = 0.086 \pm 0.019$

CHAPTER 6

DISCUSSION, CALCULATIONS AND CONCLUSIONS

From Figs. VIII and IX, several features are readily apparent. First of all, it is seen that the general angular behaviour, discussed in the theory section on quadrupole interaction, is quite definitely borne out. This allows a reasonably accurate value of the quadrupole coupling parameter A to be obtained. As seen from the tabulated values in Table 1, a slight increase is noted in the value of A as the temperature is lowered to T=77°K. A decrease in A is not expected, for if anything as the temperature decreases so does any amplitude of vibration of the oxygen atoms about their equilibrium positions, thereby strengthening the quadrupole interaction(10) Allowing for the statistical standard errors quoted for the two values, it may safely be said that there is no marked temperature dependence of A, in other words, of e^2qQ. This rules out the existence of a soft phonon mode, at 77°K, that rearranges the oxygens. Also, since the value of A is so little affected down to T=77°K, there is thus no evidence of any symmetry change in the crystal down to this temperature. If there were a symmetry change, then the value of eq, and therefore of A, would change substantially. This lack of symmetry reduction is further shown by the fact that the electric field gradient

asymmetry parameter η has value zero, so that one is observing only one vanadium site rather than, say, two inequivalent sites. Such a result is expected from symmetry considerations.

As indicated in Chapter II it is expected that the various components of the magnetic ion interaction tensor $\vec{C}$, along the special directions of interest, should scale with the magnetization $\vec{M}$ along these directions. It is seen in Table 1, however, that this is not observed. It is therefore of interest at this point to investigate a little more closely the various contributions to the interaction tensor, that is, the various contributions to the actual local field, $\vec{H}_{loc}$, at a vanadium nucleus site. The local field is a sum of four terms:

$$\vec{H}_{loc} = \vec{H}_0 + \vec{H}_1 + \vec{H}_2 + \vec{H}_3.$$

The problem is treated in the standard fashion, where the sample is in the shape of an ellipsoid of revolution or a limiting case thereof. An imaginary spherical cavity, called the Lorentz cavity, is drawn in the sample, centred on a vanadium nucleus. In this way, the terms in the above expression for H_{loc} are defined as follows. $\vec{H}_0$ is the external applied field. $\vec{H}_1$ is the so-called 'Lorentz cavity field', i.e. the field from the surface magnetization dipoles on the inside of the spherical cavity described. $\vec{H}_2$ is the 'demagnetization field' derived from a surface current density $\hat{n} \times \vec{M}$ on the outer surface of the specimen, where $\hat{n}$ is the normal to the surface. This reduces the field inside the sample, according to:

$$\vec{H}_2 = -N_i \vec{M}_i = -N_i \chi_i \vec{H}_i ,$$

where N_i is the 'demagnetization factor' for the direction 'i' of interest, and χ_i is the magnetic susceptibility along that direction. The demagnetizing field is dependent on the shape of the sample, and it will be seen that the value of this term may achieve quite large values for our particular sample geometry. $\vec{H}_3$ is the 'dipole sum' term due to the field of the atoms inside the cavity described. The fields due to these magnetic moments are summed by the Ewald method.

The relative magnitudes of these contributions must be examined in order to see if there is any dominating term. $\vec{H}_1$, in c.g.s. units, is given by:

$$\vec{H}_{1i} = \frac{4\pi}{3} \vec{M}_i \quad (11)$$

Since the sample used was a composite mosaic of nine crystals to form a parallelepiped, as described in Chapter III, the sample is not an ellipsoid of revolution. Therefore the magnetization, and thus the demagnetizing field $\vec{H}_2$ is not uniform throughout the sample, and is in fact difficult to calculate precisely. Therefore, several approximations were made in the determination of the demagnetizing factors. H_2 was first calculated assuming the sample to be an 'infinitely long thin cylinder' along the c-axis of the crystal. The values of $N_{||}$ and $N_{|}$ are then 0 and 2π respectively, for the directions $\Theta=0$ and $\Theta=\pi/2$. A second approximation used was in fact that of a finite ellipsoid of revolution with suitable

'eccentricity' or ratio of dimensions. Following the method of Bozorth and Chapin[13], it is found that:

$$N_{||} = 4\pi n_{||} = 4\pi\left(\frac{1}{e^2} - 1\right)\left(\frac{1}{2e}\ln\frac{1+e}{1-e} - 1\right),$$

and that:

$$N_{\perp} = 4\pi n_{\perp} = 2\pi\left(\frac{1}{e^2} - \frac{e^2-1}{2e^3}\ln\frac{1+e}{1-e}\right),$$

where e is the eccentricity and is given by $e=\sqrt{1-a^2/c^2}$. Two other approximations were employed, one assuming the whole sample to be a single spherical sample, the other according to a method by Sharma[14] using 'average demagnetizing factors', in order to get an idea of the relative magnitudes of the demagnetizing field for various approximating geometries. The results for these calculations are found in Table 2. Since $\sum_i n_i = 1$, it is obvious that the greatest value that $\vec{H}_2$ can achieve is $\vec{H}_2 = -4\pi\vec{M}$, with the n_i all zero for the other directions.

The dipole sum field $\vec{H}_3$ now has to be considered. The field at a vanadium site i due to all the magnetic dipole moments μj at sites j within the sphere described above, has to be calculated. The total field from all such μj's over the whole sphere may be written in the form:

$$H_i^{\alpha} = \sum_k \sum_j d_{i,jk}^{\alpha\beta}\mu_j^{\beta} = \frac{\langle\mu^{\beta}\rangle}{\Omega}\sum_j c_{ij}^{\alpha\beta},$$

where Ω is the unit cell volume, and the sum over k extends over all unit cells in the crystal. The sum over j is over the magnetic moments inside a unit cell. This expression gives the α'th component of the field at the i'th vanadium

TABLE 2

The table gives the values of the demagnetizing fields for the two directions $\vec{H}_{||}\vec{c}$ and $\vec{H}_{\perp}\vec{c}$, for T = 292°K and T = 77°K. The four approximations used for their calculations are:

(a) Long Thin Cylinder; $N_{||}=0$, $N_{\perp}=2\pi$.

(b) Prolate Spheroid; $N_{||}=1.370$, $N_{\perp}=8.545$.

(c) Sharma Interpolation; $N_{||}=1.885$, $N_{\perp}=5.341$.

(d) Sphere; $N_{||}=N_{\perp}=\frac{4\pi}{3}$.

(e) Gives the Lorentz fields for the 4 combinations of Θ and T.

	T = 292 °K		T = 77°K	
	$\vec{H}_{\parallel}\vec{c}$	$\vec{H}_{\perp}\vec{c}$	$\vec{H}_{\parallel}\vec{c}$	$\vec{H}_{\perp}\vec{c}$
(a)	0.0 Oe	-100.512 Oe	0.0 Oe	-402.050 Oe
(b)	-16.920 Oe	-136.695 Oe	-25.381 Oe	-546.779 Oe
(c)	-23.282 Oe	- 85.440 Oe	-34.922 Oe	-341.760 Oe
(d)	-51.734 Oe	- 67.008 Oe	-77.602 Oe	-268.033 Oe
(e)	+51.734 Oe	+ 67.008 Oe	+77.602 Oe	+268.033 Oe

nucleus due to all the β'th components of the Dy^{3+} magnetic moments within the sphere. The magnetization M is given by:

$$M^{\beta} = 2\frac{<\mu^{\beta}>}{\Omega} \text{ emu/unit volume},$$

where $<\mu^{\beta}>$ is the thermal average dipole moment on a Dy^{3+} ion in the β-direction. Thus:

$$H_i^{\alpha} = \frac{M}{2} A_i,$$

where $A_i = \Sigma_j c_{ij}^{\alpha\beta}$ is the dipole sum coefficient for the α'th component of H_i. The coefficients $c_{ij}^{\alpha\beta}$ were calculated using a computer program written by E. R. Cowley. His program employs the Ewald method to evaluate the sums. Also, as the magnetic field from a dipole decreases as r^{-3}, it cannot be assumed that the Dy^{3+} ion is a point dipole, but rather, say, a distribution over the finite volume of the ion. That is, there is a possibility of contributions from higher-order magnetic multipoles. Therefore, in performing the dipole sum calculation, several spacial distributions of the Dy^{3+} magnetic dipole moment were investigated. The moment was 'subdivided' into a central ion surrounded by 2 or 4 satellite ions, with the total μ_{Dy} being distributed amongst these ions. The results for the extreme cases are given in Table 3.

Summing the values of H_1, H_2, and H_3, and comparing these values with those expected from the parameters C_{XX} and C_{ZZ}, one sees that there is a discrepancy of at least 200 Oe. An explanation of this lack of agreement between the values of C_{XX} and C_{ZZ} and those of M_{XX} and M_{ZZ} must therefore be looked for. A possible mechanism which has not yet been

TABLE 3

The table gives the values of the dipole field for the two directions $\vec{H}_{||}\vec{c}$ and $\vec{H}_{\perp}\vec{c}$ for T = 292°K and T = 77°K. These are based on the assumptions that there are:

(i) 1 central and 4 satellite Dy^{3+} in the a-b plane. The magnetic moment is shared equally between the 4 satellites only.

(ii) 1 central and 4 satellite Dy^{3+} ions in the a-b plane. The magnetic moment is all attributed to the central ion.

(iii) 1 central and 2 satellite Dy^{3+} ions along the c-direction. The magnetic moment is shared equally between the 2 satellites only.

(iv) 1 central and 2 satellite Dy^{3+} ions along the c-direction. The magnetic moment is all attributed to the central ion.

(v) gives the Lorentz fields for the 4 combinations of Θ and T.

	T = 292°K		T = 77°K	
	$\vec{H}_{\parallel}\vec{c}$	$\vec{H}_{\perp}\vec{c}$	$\vec{H}_{\parallel}\vec{c}$	$\vec{H}_{\perp}\vec{c}$
(i)	+219.267 Oe	-141.998 Oe	+328.892 Oe	-567.990 Oe
(ii)	+ 76.938 Oe	- 49.825 Oe	+115.405 Oe	-199.301 Oe
(iii)	+285.671 Oe	-185.000 Oe	+428.495 Oe	-740.001 Oe
(iv)	+ 76.938 Oe	- 49.825 Oe	+115.405 Oe	-199.301 Oe
(v)	+ 51.734 Oe	+ 67.008 Oe	+ 77.602 Oe	+268.033 Oe

explicitly taken into account is the transferred hyperfine (TH) interaction between the Dy^{3+} ions and the vanadium nuclei. This TH interaction results in an effective fractional spin transfer from the Dy^{3+} ions to the vanadium ions. Considering the Dy^{3+} ion, one would at first consider the 4f electrons to be well shielded, so that the TH interaction, if any, might be considered to be too small to be worth including. However, one can perform an order of magnitude calculation to show that in fact the TH interaction may be a cause of the discrepancies noted above. So far, $\vec{H}_{loc}$ has only included terms which scale with the magnetization $\vec{M}$, i.e. with $\langle\vec{\mu}\rangle$. $\vec{H}_{loc}$ could be written then as:

$$\vec{H}_{loc} = \vec{H}_0(1 + \alpha_1 + \alpha_2 + \alpha_3),$$

and it would be expected that the components of $\vec{c}$ would scale with the corresponding components of $\vec{M}$. It is seen that they do not. Now, the TH interaction may be written as:

$$H_{TH} = \vec{I}\cdot\vec{A}\cdot\langle\vec{S}\rangle,$$

where $\langle\vec{S}\rangle$ is not directly measurable and must be calculated. The calculation involves extensive knowledge of the energy levels and wavefunctions of the Dy^{3+} ion. The magnetic moment has contributions from both $\langle\vec{S}\rangle$ and $\langle\vec{L}\rangle$. In general, the temperature dependence of $\langle\vec{S}\rangle$ and $\langle\vec{\mu}\rangle$ can be quite different. As a result, the TH interaction will not necessarily scale with $\langle\vec{\mu}\rangle$, i.e. with $\vec{M}$.

Electron paramagnetic resonance (EPR) experiments performed on rare-earth ions substituted into isomorphous YVO_4[15] have found EPR resonances of line widths not greater than 10 to

15 Oe. An accurate calculation of the TH interaction is beyond the scope of this work, but should an order of magnitude calculation yield a value not too far from the EPR measured line widths, this would suggest that the TH interaction might exist and might therefore resolve the discrepancies.

In order to simplify the calculation, it is assumed that $I=\frac{1}{2}$ for ^{51}V and that $\langle\vec{S}\rangle$ is given by $\frac{\mu_\beta H}{k_B T}$, where μ_β is a Bohr magneton, H is 10 kOe, and k_B is Boltzmann's constant. One may look at the TH interaction from two points of view. Firstly, looking at the effect of the Dy^{3+} ion on the vanadium nucleus, one equates:

$$I \cdot A_{TH} \cdot \langle S \rangle \simeq 200 . \mu_V ,$$

where the number 200 represents the discrepancy in Oe and μ_V is the ^{51}V nuclear magnetic moment. Then $I \cdot A_{TH} \cdot \langle S \rangle \simeq 5.2 \times 10^{-21}$ ergs. Setting $I=\frac{1}{2}$ and $\langle S \rangle = \frac{\mu_\beta H}{k_B T}$, we have that:

$$A_{TH} \simeq 10.4 \times 10^{-21} \times \frac{k_B T}{\mu_\beta H} .$$

Looking now at the TH interaction from the point of view of the effect of the ^{51}V nucleus on the Dy^{3+} ion, that is, looking at the EPR experiment, it is shown that the separation factor A_{TH}, in field units, will be given by:

$$A_{TH} \simeq \frac{10.4 \times 10^{-21}}{\mu_\beta} \cdot \frac{k_B t}{\mu_\beta H} \simeq 400 \text{ Oe},$$

taking only orders of magnitude. Allowing for factors of 2 or

3, it is seen that, although larger, A_{TH} is of the same order of magnitude as the EPR linewidth of 15 Oe quoted above. Thus it is conceivable that the TH interaction plays a role in the value of $\vec{H}_{loc}$ and might possibly explain why the parameters C_{XX} and C_{ZZ} do not scale with $M_{\perp}$ and $M_{||}$.

It is of interest to suggest what might be expected to happen to the values of the parameters C_{XX}, C_{ZZ}, and A in the very low temperature range of 2.0°K to 15.0°K. This is the temperature range where, decreasing the temperature, the $DyVO_4$ crystal first goes through a spontaneous crystallographic distortion accompanied by a symmetry reduction, at T_D = 14°K, and then goes through the Neel transition to an antiferromagnetic ordering state below 3.04°K. The Jahn-Teller distortion produces a lowering of the crystal symmetry, which would obviously cause the value of A to change, since the field gradient eq = V_{ZZ} would be altered. If axial symmetry no longer holds, then all vanadium sites are no longer necessarily equivalent, and the asymmetry parameter η would not be zero. The latter would be borne out in the NMR spectrum which would show, say, two signals for each transition m↔m-1 if there are two 'inequivalent' sites. The values of C_{XX} and C_{ZZ} would increase by virtue of the increase in magnetization along the appropriate directions at these low temperatures. Below T_N=3.04°K, the values would depend on the details of the antiferromagnetic ordering.

In summary, then, it can be said that the results obtained in these experiments have shown that there is no

alteration of crystal symmetry in $DyVO_4$ in going from room temperature to that of liquid nitrogen. The values of the parameters A=-0.0479±0.0002 at T=292°K and A=-0.0495±0.0005 at T=77°K, as well as η=0 for the both temperatures, have shown this to be the case. Dipole sum calculations performed with distributions of the total Dy^{3+} magnetic moment have shown that multipole moments higher than the dipole moment of the Dy^{3+} ion contribute very little, if anything, to the local field at the vanadium nucleus. It is seen, too, that contrary to expectations, the parameters C_{XX} and C_{ZZ} do not scale with the magnetizations $M_{\perp}$ and $M_{||}$, respectively, as the temperature is reduced from T=292°K to T=77°K. This is not at present completely understood, although it may well be that the transferred hyperfine interaction can provide an explanation for the discrepancy.

REFERENCES

1. Bohm, W., Herb, R., Kahle, H. G., Kasten, A., Laugsch, J., and Wuchner, W., phys. stat. sol.(b) 54, 527 (1972).
2. Becker, P.-J., Dummer, G., Kahle, H. G., Klein, L., Muller-Vogt, G., and Schopper, H.C., Phys. Letters (Netherlands) 31A, 499 (1970).
3. Wuchner, W., Bohm, W., Kahle, H. G., Kasten A., and Laugsch, J., phys. stat sol. (b) 54, 273 (1972).
4. Cooke, A. H., Martin, D. M., and Wells, M. R., "The Specific Heat of $DyVO_4$", The Clarendon Laboratory, Parks Road, Oxford.
5. Fuess, H., Kallel, A., J. Sol. State Chem. 5, 11 (1972).
6. Will, G. and Schafer, W., J. Phys. C:Sol. State Phys. 4, 1971.
7. Kopfermann, H.,"Nuclear Moments", Academic Press, Inc. New York (1958).
8. Choh, S. H. and Stager, C. V., "Nuclear Magnetic Resonance Studies of $K_2CuCl_4 \cdot 2H_2O$", 49, #1 (1971). Published by the National Research Council of Canada.
9. Abragam, A., "The Principles of Nuclear Magnetism; The International Series of Monographs on Physics"; Oxford University Press, London (1961).

10. Cohen, M. H. and Reif, F., "Quadrupolar Effects in Nuclear Magnetic Resonance Studies of Solids" Solid State Physics 5, Academic Press, Inc., New York (1957).

11. Drain, L. E., Met. Reviews, 119 (1967).

12. Fiegelson, H. S., J. Amer. Ceram. Soc. 47, 257 (1964).

13. Bozorth, R. M., and Chapin, D. M., J. Appl. Phys. 13, 320 (1942).

14. Sharma, P.V., Geophysics (USA) 33, #1, 132 (1968).

15. Owen, J. and Thornley, J.H.M., Rep. Prog. Phys. Vol. VI, 29, 675 (1966).

16. Andrew, E.R., "Nuclear Magnetic Resonance' Cambridge Monographs on Physics", Cambridge Univ. Press (1956).